AD_____

Award Number: W81XWH-11-2-0064

TITLE: Preventing Vision Loss from Blast Injuries with Regenerative Biomaterial

PRINCIPAL INVESTIGATOR: Brian D. Lawrence, Ph.D.

CONTRACTING ORGANIZATION: Sarentis Ophthalmics, Inc.
Eagan, MN 55123

REPORT DATE: August 2013

TYPE OF REPORT: Final

PREPARED FOR: U.S. Army Medical Research and Materiel Command
Fort Detrick, Maryland 21702-5012

DISTRIBUTION STATEMENT: Approved for public release; distribution unlimited

The views, opinions and/or findings contained in this report are those of the author(s) and should not be construed as an official Department of the Army position, policy or decision unless so designated by other documentation.

REPORT DOCUMENTATION PAGE

Form Approved
OMB No. 0704-0188

1. REPORT DATE *(DD-MM-YYYY)*	2. REPORT TYPE	3. DATES COVERED *(From - To)*
August 2013	Final	30 November 2010 - 31 July 2013

4. TITLE AND SUBTITLE
Preventing Vision Loss from Blast Injuries with Regenerative Biomaterial

5a. CONTRACT NUMBER

5b. GRANT NUMBER
W81XWH-11-2-0064

5c. PROGRAM ELEMENT NUMBER

6. AUTHOR(S)
Brian D. Lawrence, Ph.D.

E-Mail: BLAWRENCE@SERYXBIOMEDICAL.COM

5d. PROJECT NUMBER

5e. TASK NUMBER

5f. WORK UNIT NUMBER

7. PERFORMING ORGANIZATION NAME(S) AND ADDRESS(ES)
Sarentis Ophthalmics, Inc.
Eagan, MN 55123

8. PERFORMING ORGANIZATION REPORT NUMBER

9. SPONSORING / MONITORING AGENCY NAME(S) AND ADDRESS(ES)
U.S. Army Medical Research and Materiel Command
Fort Detrick, Maryland 21702-5012

10. SPONSOR/MONITOR'S ACRONYM(S)

11. SPONSOR/MONITOR'S REPORT NUMBER(S)

12. DISTRIBUTION / AVAILABILITY STATEMENT
Approved for Public Release; Distribution Unlimited

13. SUPPLEMENTARY NOTES

14. ABSTRACT

Millions of Americans suffer from ocular trauma annually, in which military personnel are at an increased risk of experiencing such injury due to their operating environment. Seryx Biomedical in collaboration with the Weill Cornell Medical College has developed an ocular bandage produced from silk protein, which self-adheres to the eye's surface and aids in stimulating the wound healing process. During the award period the silk bandage design and manufacturing process was defined from raw material source to packaged product for use in animal pre-clinical trials. In vitro work has indicated that the silk protein is not toxic, promotes cellular wound healing migrations, and inhibits the inflammation process. Results from in vivo rabbit animal models have indicated that the silk bandage can enhance corneal healing by 33%, and is largely dictated by the potential residence time of the device upon the corneal surface. Additionally, processing of the silk material is critical for producing consistent material properties, which were controlled by implementing novel systems for producing the silk solution and thus reducing material variability. All taken together the work performed during the award period has indicated that silk biomaterials offer great potential for use in healing the ocular surface after traumatic injury, and that further development of silk-based ophthalmic products is warranted and will continue.

15. SUBJECT TERMS
None provided.

16. SECURITY CLASSIFICATION OF:			17. LIMITATION OF ABSTRACT	18. NUMBER OF PAGES	19a. NAME OF RESPONSIBLE PERSON
a. REPORT	b. ABSTRACT	c. THIS PAGE			USAMRMC
U	U	U	UU	29	19b. TELEPHONE NUMBER *(include area code)*

Table of Contents

1.0: Introduction

Seryx Biomedical, Inc., in collaboration with the Weill Cornell Medical College is developing a novel regenerative biomaterial derived from the silk protein fibroin from the *Bombyx mori* silkworm. This will be the first ophthalmic product that utilizes regenerative silk protein for use on the ocular surface. Over 6 million Americans sustain traumatic injuries each year from both accidents and surgical procedures. In addition, eye injury is the number one cause of field evacuation in the military. Corneal wounds cause intense pain and may lead to blindness depending on the severity of injury. Seryx's regenerative biomaterial accelerates corneal healing and soothes the damaged surface by providing a coating over the injury site. In addition, work from this award has demonstrated the protein also possesses anti-inflammatory properties. This regenerative material is a renewable resource, inexpensive to manufacture, and can be produced utilizing a fully scalable GMP process. As a result silk fibroin protein offers much promise for future biomaterial applications in ophthalmology and also in a broader biomedical context.

2.0: Body

2.1: Irritation response to silk films

2.1.1: Irritation response to silk protein *in vitro*

Previous research has demonstrated that silk fibroin protein derived from the *Bombyx* mori silkworm cocoon is not toxic and non-immunogenic when placed within the body (*1*). It is also known that silk fibroin possesses anti-inflammatory properties (*2*). In an effort to verify these reports the irritation response to silk protein in solution was evaluated *in vitro* on an immortalized human corneal-limbal epithelial (HCLE) cell line. HCLE cells were grown to confluence in culture, and the media was then supplemented with various concentrations of silk fibroin protein solution. A scratch wound was then produced upon the cell culture surface, and the time for the cultures to regrow over the wounded culture area was observed using time-lapse phase-contrast imaging over a 15-hour period as previously described (*3*). Results indicated that samples treated with silk protein healed significantly faster than phosphate buffered saline (PBS) controls (Figure 1A-B). It was found that by 10-hours in culture the silk treated samples were 99% healed compared to 66% healed controls (Figure 1C). This resulted in a near 50% increase in healing rate for the silk treated groups, and was statistically significant ($p<0.05$) as determined by student t-test analysis.

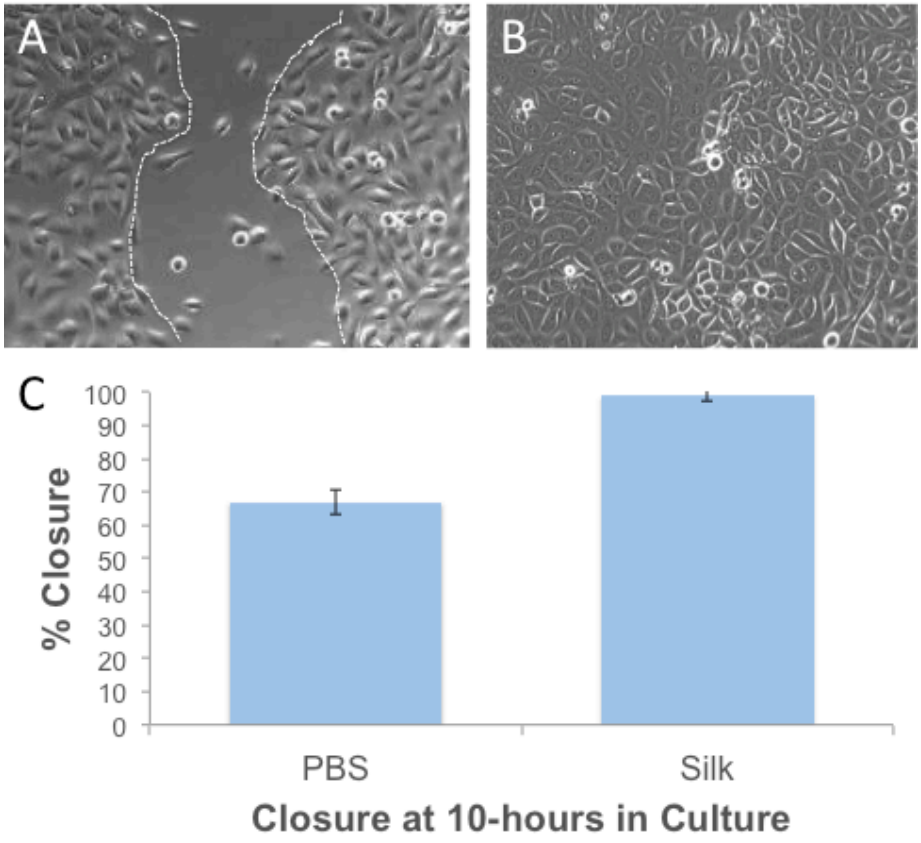

Figure 1. Selected phase contrast images from time-lapse movies for HCLE cultures at 10-hours post-wound creation for (A) controls treated with PBS and (B) silk treated cultures respectively. (C) Analysis indicated a near 35% increase in wound area closure by 10-hours post-wound induction for silk treated cultures (n = 9, $p<0.05$, error bars indicate standard deviations).

The *in vitro* observations indicate that the silk protein in solution is not toxic and significantly enhances wound-healing rate. The wound healing studies were then followed up using a p65 assay to assess the potential for anti-inflammatory properties (*4*). The nuclear transcription factor p65 is part of the NF-kB complex. When p65 is activated it translocates into the nucleus and activates a number of inflammatory genes, which leads to cytokine production that act to stimulate inflammation. As a means to test the inflammatory nature of the silk protein on HCLE cells p65 activation was assessed.

Confluent HCLE cell cultures were treated with PBS, hyperosmotic media, and two concentrations of silk in hyperosmotic media (Figure 2). Hyperosmotic media is known to produce an inflammation response through the NF-kB pathway for corneal-derived cells, therefore hyperosmotic media conditions were used to stimulate cellular

inflammatory pathways for HCLE cells. Staining of p65 was located primarily in the cytoplasm for untreated controls, which is the expected response for cells in a non-inflammatory state (Figure 2A). However, the p65 staining was relegated to the nucleus for cells in hyperosmotic media indicating inflammatory pathway activation (Figure 2B). Interestingly, p65 staining for cells treated with silk was largely in the cytoplasm and demonstrated a dose dependent response possessed more nuclear staining at lower concentrations (Figure 2C-D). These results indicate that the silk fibroin protein is eliciting an anti-inflammatory property upon HCLE cells dose dependently. These results in combination with the scratch assay data provide evidence that silk protein is non-toxic, regenerative, and provides anti-inflammatory effects *in vitro*.

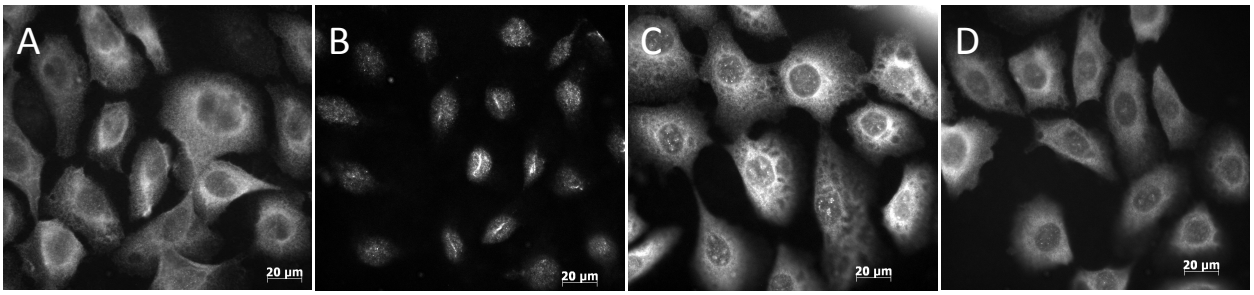

Figure 2. p65 staining for HCLE cells cultured in varying conditions: (A) PBS, (B) hyperosmotic media, (C) hyperosmotic media with low concentration silk fibroin, and (D) hyperosmotic media with high concentration silk fibroin.

2.1.2: Silk bandage application to rabbit cornea

The silk solution was then formed into a corneal bandage device, described in more detail below in section 2.5, and then assessed for acute toxicity upon the rabbit cornea. The curved bandage was designed to fit the curvature of the rabbit eye, which is largely considered to be the optimal choice for pre-clinical assessment of new ophthalmic therapies (*5*). It was shown that the curved silk film bandage could be readily applied to the rabbit's eye, which was then monitored using slit lamp photography (Figure 3). The silk bandage was found to be mucoadhesive by adhering to the cornea's epithelial surface, which then flattened over the curved cornea surface while remaining attached and dissolved with time.

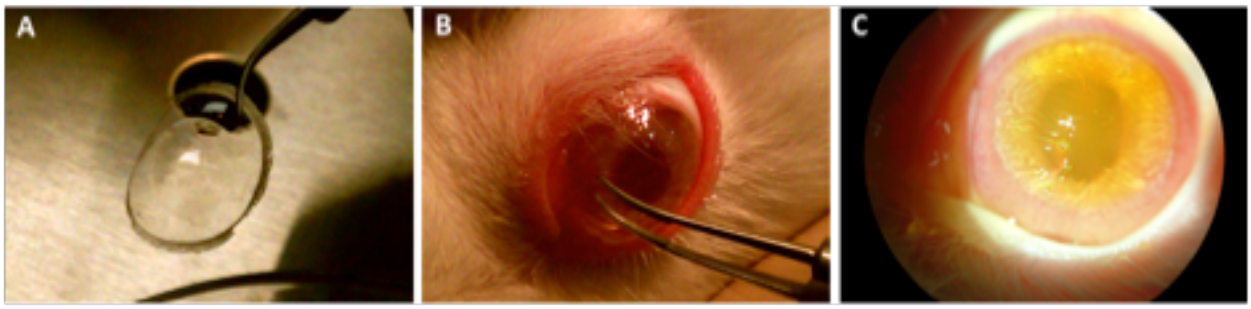

Figure 3. (A) The silk film bandage is administered using forceps, (B) applied directly to the rabbit cornea, and (C) then observed using slit lamp photography.

Optical coherence tomography was used to assess silk film mucoadhesive attachment to the corneal surface (Figure 4). Upon initial application of the processed bandages the material adhered to the corneal surface and began to immediately swell in thickness. Wave morphologies were observed with material cross-sectional thickness ranging from 79 to 114-μm (Figure 4A-B). After 1 minute post-application the silk bandage thickness had flattened out to around 100-μm, which corresponded to a 25% increase in bandage thickness (Figure 4C). Over a 3-minute time period the thickness increased up to 136-μm, which corresponded to a 70% increase (Figure 4D-E). The thickness then began to decrease as the material started to dissolve after 4-minutes post application (Figure 4F). After 10-minutes post-application the silk bandage thickness had reduced to around 100-μm in thickness, and the edge regions appeared to maintain both consistent thickness and attachment to the corneal surface (Figure 4G). After a total of 45-minutes upon the eye portions non-dissolved particulates were observed on the cornea surface in various locations (Figure 4H). The rabbit cornea appeared unaffected by the presence of the material, and the animal showed no signs of discomfort or subsequent inflammation after the silk bandage's application. These results indicate that the silk bandage is attaching to the cornea surface and absorbing fluid upon application. The material then hydrates and swells into a gel-like state, which then uniformly coats the surface and begins to dissolve with time. The bulk of the silk bandages appeared to dissolve within 45-minutes post-application.

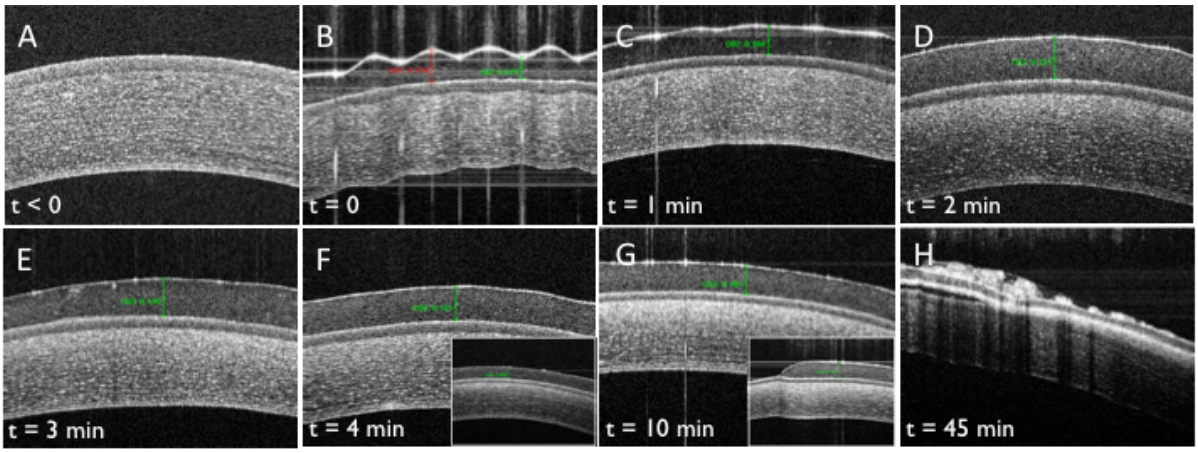

Figure 4. The silk bandage's initial adhesion to the (A) cornea was evaluated over time with OCT imaging from (B-F) 0 to 4-minutes, (G) 10-minutes, and (H) 45-minutes respectively. (B) The bandage was found to form wave morphologies upon initial adhesion, (C-E) then swelled as the material hydrated. (F-G) This was followed by a period of material dissolution as the bandage reduced in thickness. (G) The bandage edge showed uniform thickness and remained well adhered to the corneal surface after 10-minutes post application. (H) Insoluble portions of the silk bandage were measured at 45-minutes showing the remaining silk particulates.

2.1.3: Silk bandage toxicity assessed through histological examination

Silk bandages were applied to the rabbit eye, and then examined via slit lamp microscopy for evidence of ocular surface infection, ulceration, or cellular infiltrate, as well as for any evidence of intraocular inflammation over a 1-week period. By all metrics, eyes receiving silk bandages as well as untreated controls were consistently found to be absent of inflammation. Eyes from animals receiving silk films and also untreated controls were harvested from rabbits and evaluated histologically (Figure 5). Masked evaluation of samples demonstrated no evidence of detrimental effects from the application of silk bandages (Figure 5B). Application of silk films did not lead to corneal stromal loss, corneal melt, delay in epithelialization, or increased numbers of inflammatory cells.

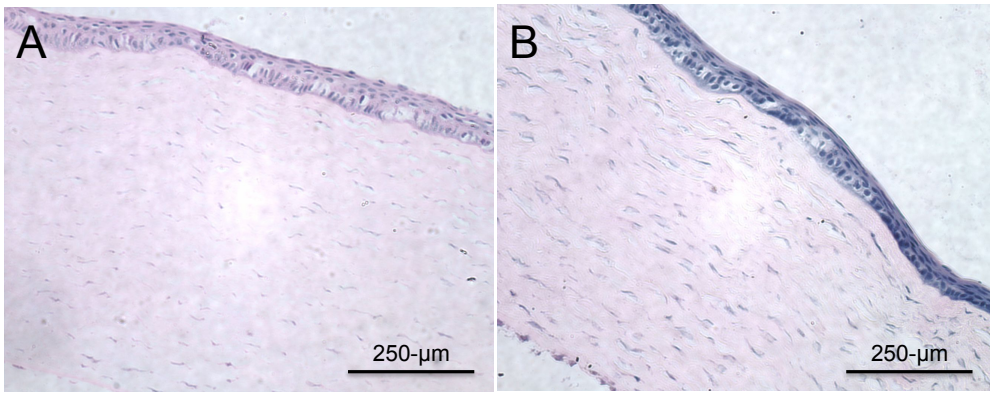

Figure 5. Corneal surface that were (A) untreated controls and (B) treated with silk film bandages. Histology results indicate the silk material produced no adverse reactions with the rabbit corneal tissue.

2.2: Abrasive wound assessment

2.2.1: Short dissolution time silk bandage assessment

Rabbit animal trials demonstrated that treatment of a denuded epithelial corneal surface with silk film biomaterial enhanced the observed 24-hour healing rates in rabbits. An epithelial debridement rabbit animal model was developed to simulate the surgical injury performed during a photorefractive keratectomy (PRK) procedure, which can then be used to monitor epithelial healing rates and assess the rabbit cornea's initial response to the application of the silk bandage material (*3*). A silk bandage was produced aseptically by casting silk solution onto a 14 mm diameter silicone rubber substrate, air-dried overnight, and air lifted from the mold using forceps (*6*).

The corneal epithelial debridement surgeries were performed, and then silk bandages were applied to the injury bed of the "treated" group of animals (n = 3). The corneal wounds were then followed using fluorescein dye, which indicates a de-epithelialized surface as denoted by green fluorescence under blue light (Figure 6A). Animals were monitored until complete epithelial healing was reached (48-72 hours) as indicated by lack of fluorescein staining. Silk film bandages dissolved on the ocular surface within five minutes after application, and demonstrated no effect on healing when compared to the controls (Figure 6B-C). From this result, it was demonstrated that the material caused no adverse effect on healing. It was hypothesized that a longer residence time upon the cornea may promote healing to a greater extent.

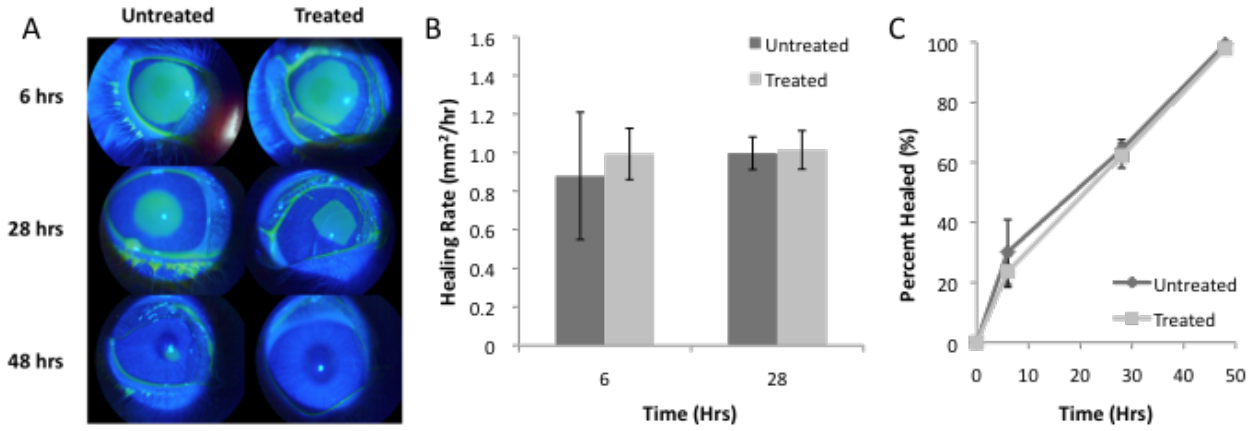

Figure 6. (A) Fluorescein staining images of rabbit cornea healing progression for treated and untreated rabbits over a 48-hour period. (B) Healing rate and (C) percent healed data comparing silk film bandage treated and untreated rabbits for the epithelial debridement injury model.

2.2.2: Characterization of water-annealed (WA) silk film dissolution rate

The water-annealing (WA) process was implemented in an attempt to prolong silk bandage dissolution rate upon the rabbit cornea surface. WA processing is a common silk film treatment method that extends the dissolution time of the material by increasing hydrogen bonding within the material through beta-sheet secondary structure formation (*7*). To aid in eliminating potential variability produced from the WA environment a more sophisticated environmental glove box chamber was designed and fabricated (Figure 7A). The chamber controls temperature within 0.3°C and relative humidity within 2% variation (Figure 7B). The chamber is equipped with sealed glove ports that will allow handling of materials within the processing chamber without risk of compromising the internal environment. The additional environmental control allows for a predictable and reproducible processing regime, and has ample space for production (Figure 7C).

A.

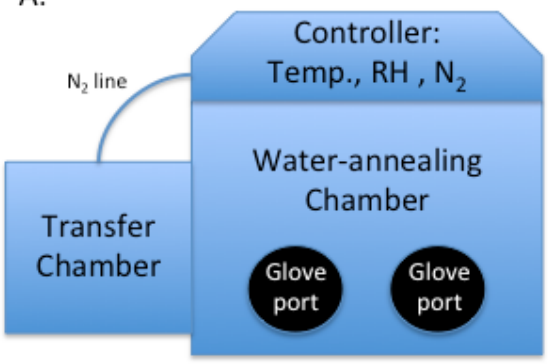

B.

Environmental Control Specifications			
Temperature		**Humidity**	
Temperature Range:	16-41° C	Humidity Range:	1-95% Rh
Temperature Sensor:	±0.3° C	Humidity Sensor:	±2% Rh
Resolution:	±1°	Control Accuracy:	±1% Rh
On Screen Datalogging:	0.1° C	Resolution:	0.1% Rh

C.

Physical Dimensions	
I.D.	28"w x 23"d x 29"h
O.D.	43"w x 30"d x 43"h
Top Opening	17" x 23"
Door Opening	15"w x 18"h
Chamber Vol.	11.2 cu. ft.
Weight	250 lbs.

Figure 7. (A) Schematic of the WA processing apparatus design consisting of a transfer chamber, WA chamber, and controller. (B) Specifications table listing important environmental control features of the design. (C) Listing of physical dimensions of the design.

Utilizing the environmental chamber, initial experiments were performed that processed the silk bandages at varying temperature (16-65°C) at dew point saturation (100% RH). Samples were then processed for 0-60 minutes within the environmental chamber and then removed for analysis. Results confirmed earlier experimental observations that by changing either temperature or processing time the silk fibroin material secondary structure and dissolution within water can be modulated (*7*). FTIR analysis revealed a change in silk fibroin protein secondary structure confirmation with a more prevalent beta-sheet peak formation at 1624 cm^{-1} with increasing processing temperature and after 60 minutes of processing time (Figure 8A). Enhanced beta-sheet formation correlates to increased material dissolution time (*8*), which was believed to also indicate increased corneal residence time. Unprocessed control samples do not contain this beta-sheet peak. The formation of additional beta-sheets as observed in the FTIR spectrum corresponded to changes in silk bandage material dissolution in water (Figure 8B). Results indicate that lower temperature processing at 16°C preserved high solubility of the material within water even after 1 hour of processing time, similar to unprocessed controls (i.e. 0 minutes). However, increasing the processing temperature to 17°C resulted in a significant decreases in material solubility that was also noted for 18°C and 19°C processing temperatures. These results together agree with previous results, which demonstrate that material dissolution in water may be altered by changing either processing temperature or time.

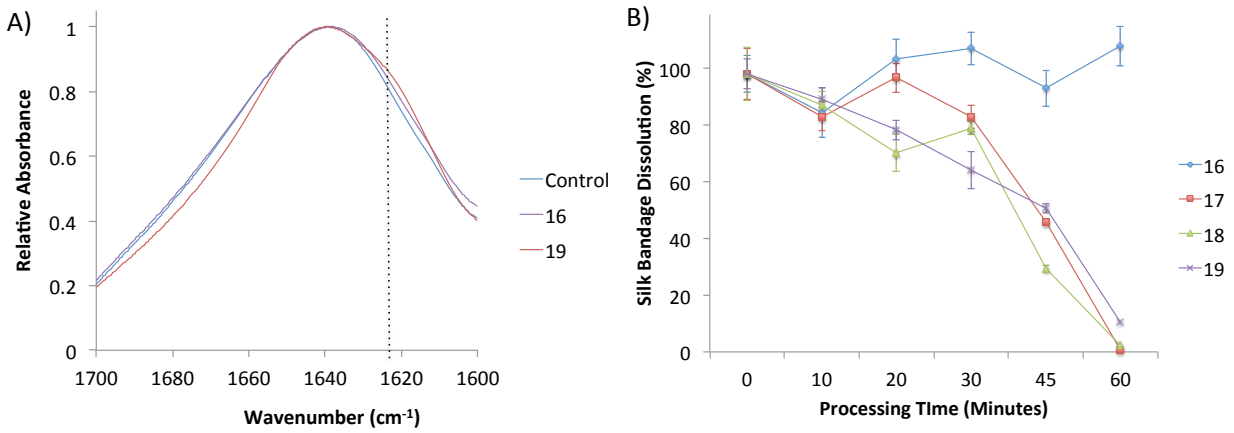

Figure 8. (A) An increase in the major silk protein beta-sheet spectral peak is observed at 1624 cm^{-1}. (B) Corresponding changes in total silk bandage sample dissolution in water with changing processing temperature and time was observed with both increased processing temperature (°C) and time.

2.2.3: *In vivo* assessment of WA films

Silk film bandages were produced using the process described above using an approximate 20-minute WA time at ambient temperature. This additional processing resulted in a near 10-fold increase in silk bandage dissolution time, which allowed the silk bandage material to remain on the eye for up to 10 hours. The corneal epithelial debridement procedure was performed and tracked over time with fluorescein staining (Figure 9A). The silk bandage treated group demonstrated a significant increase (30%, n =3) in healing rate over the first 20 hour period while the film was still present on the wound bed when compared to untreated controls (Figure 9B-C). Once the film had dissolved from the corneal surface it was shown that the healing rate was similar to untreated controls.

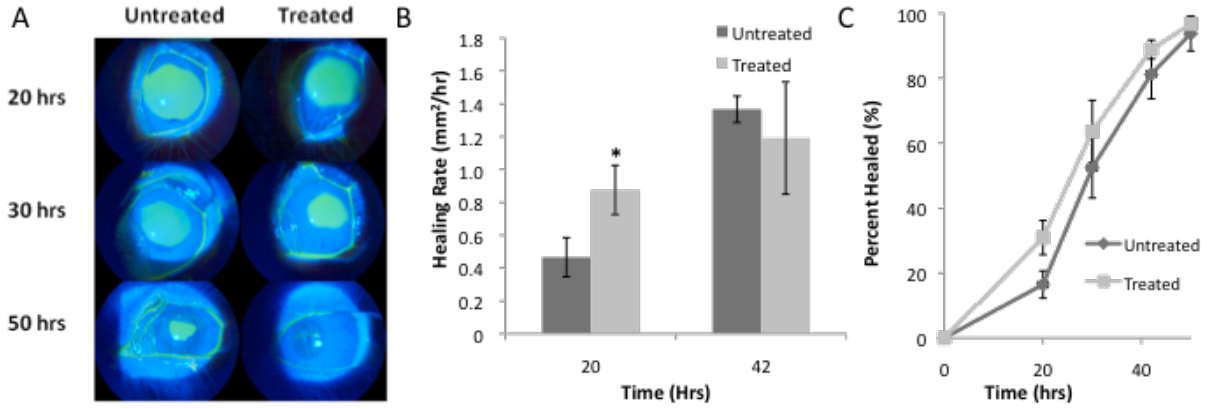

Figure 9. (A) Time course images of fluorescein stained epithelial debridement area for untreated and silk film bandage treated rabbit groups. (B) A statistically significant increase in healing rate was demonstrated over the first 20 hours post-procedure for treated animals when compared to untreated controls. (n=3, error bars indicate standard deviation, *indicates $p < 0.05$ compared to untreated controls) (C) Wound healing profile demonstrated enhanced healing profile on average for treated animals over 40 hour period post-procedure.

Epithelial debridement studies were undertaken to assess the affect that non-dissolving vs. dissolving silk film bandages have on corneal epithelium healing. Non-dissolving silk film bandages were compared to films that had extended residence time or rapid dissolution time collectively. Non-dissolved films were found to negatively impact healing rate when compared to dissolvable films, especially at time points at 24-hours and longer (Figure 10). As a result it was concluded that non-dissolving silk bandages caused adverse effects on corneal healing, most likely due to a mechanical disruption of the healing corneal epithelium. These conclusions indicated that less than 24 hour silk film bandage dissolution is an important material property for stimulating the healing process.

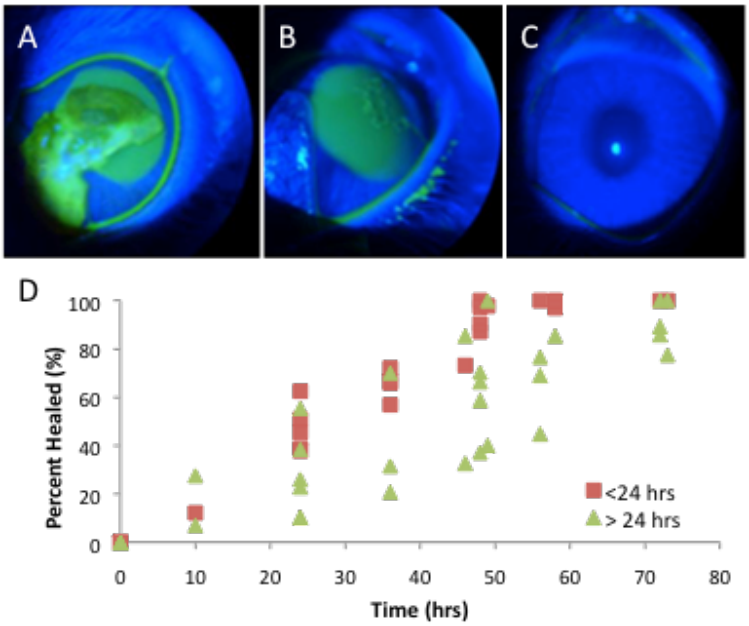

Figure 10. Fluorescein staining of debrided rabbit corneal epithelium for eyes with silk film bandages that are (A) non-dissolving (24-hours post procedure), (B) enhanced residence time (10 hours post procedure), and (C) completely dissolved (48 hours). (D) Collective scatter plot comparing percent healing for non-dissolving (green) and dissolving (red) silk film bandages.

2.3: Burn wound assessment

Evaluation of silk films in the alkali models and found that the bandages were adherent and well tolerated on the acutely burned ocular surface. A rabbit alkali injury model was developed to assess the rabbit cornea's initial response to the application of the silk film bandage material. Bandages were produced as described above. A corneal alkali injury was created upon the rabbit ocular surface, and then a silk bandage was applied to each injury bed of the treated group of animals (n = 3). The corneal wounds were then followed using fluorescein, which indicates a de-epithelialized surface as denoted by green fluorescence under blue light (Figure 11A). Animals were monitored until complete epithelial healing was reached by 72 hours as indicated by lack of fluorescein staining. These silk bandages dissolved on the ocular surface within 1 hour after initial application, and demonstrated no detrimental effect on healing when compared to the controls (Figure 11B-C). From this result, it was decided that additional processing would be needed to optimize the dissolution time upon the cornea for possible improvement in corneal recover from the alkali injury.

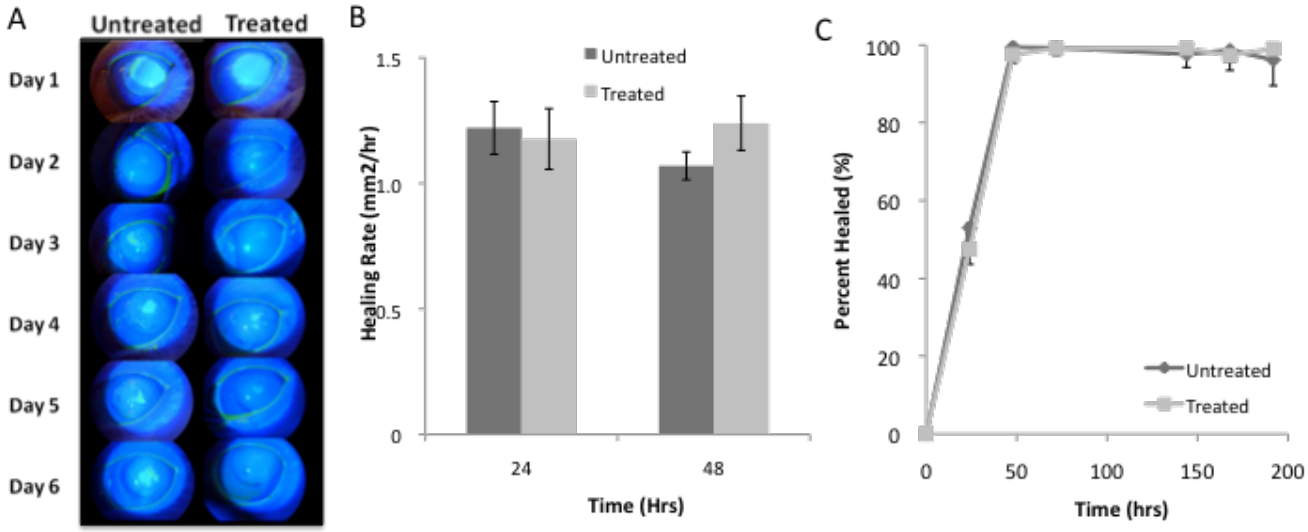

Figure 11. (A) Fluorescein staining images of rabbit cornea healing progression for treated and untreated rabbits over a 6-day period. (B) Healing rate and (C) percent healed data comparing silk film bandage treated and untreated rabbits for the alkali injury model (n = 4, error bars = standard deviation).

2.4: Puncture wound assessment

2.4.1: Intrastromal corneal toxicity

Before moving forward on puncture wound closure assessment, studies were conducted to assess the potential toxicity that the silk fibroin protein may have on corneal tissue. This is especially a concern with relation to puncture wounds, as there is the potential that non-dissolved silk protein may reside in the wound site for extended periods of time and produce undesired consequences. To explore this potential toxicity effect, the silk material was placed intrastromally within the rabbit cornea. To do this, silk films with a 6-mm diameter and a 3-μm thickness were prepared and then WA for 4-hours to produce an insoluble film sample representative of non-dissolved silk bandage material. The silk film physical dimensions were chosen to maximize the amount of implanted material by minimizing potential effects that could stem from the reduction of oxygen and nutrients to the cornea by keeping the material thin while covering the majority of the cornea area. The silk films were implanted into the anterior segment of the rabbit cornea by producing a 8-mm diameter and 150-μm depth tissue flap with a surgical blade. The film was then placed on the stroma bed, and then recovered by the flap (Figure 12).

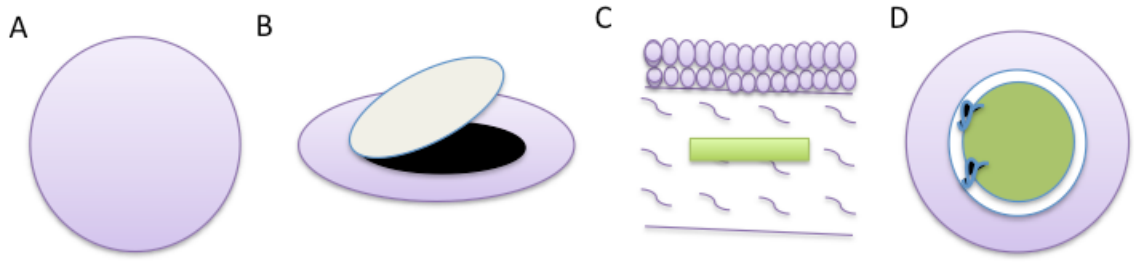

Figure 12. (A) The rabbit corneal anterior segment was partially excised by creating a (B) tissue flap. (C) The silk film was then placed within the stroma matrix, and (D) the flap was sutured closed.

Postoperative ocular inflammation, neutrophil infiltration, corneal wound healing, neovascularization, infection and integrity of the silk film were examined using a slit lamp microscope (Figure 13A-D). Corneal reepithelialization was completed within 1 week post-op with no apparent inflammatory response observed (Figure 13A). The cornea remained transparent and free from inflammation at both 4 (Figure 13B) and 12 weeks (Figure 13C) post-surgery, which compared favorably to controls (Figure 13D).

In vivo corneal architecture was examined by optical coherence tomography (OCT) at 12 weeks post-surgery, which revealed normal tissue structure and absence of inflammation (Figure 13E). Rabbits with and without silk implants were sacrificed at 1 and 3 months respectively. H&E staining of corneal histology sections was performed to examine the corneal structure, inflammatory response, and silk film degradation (Figure 13F-H). The silk film remained transparent and still present in the cornea tissue 4 weeks post-surgery (Figure 13F). The silk films appeared to integrate and degrade within the stroma matrix after 3 months with no sign of inflammation (Figure 13G), which compared favorably to controls (Figure 13H). These results indicate that the silk bandage material does not produce a toxicity response upon long-term exposure to the cornea tissue. Furthermore, it is reasonable to assume that embedment of non-dissolved bandage particulates within a puncture wound injury will not adversely affect corneal tissue homeostasis.

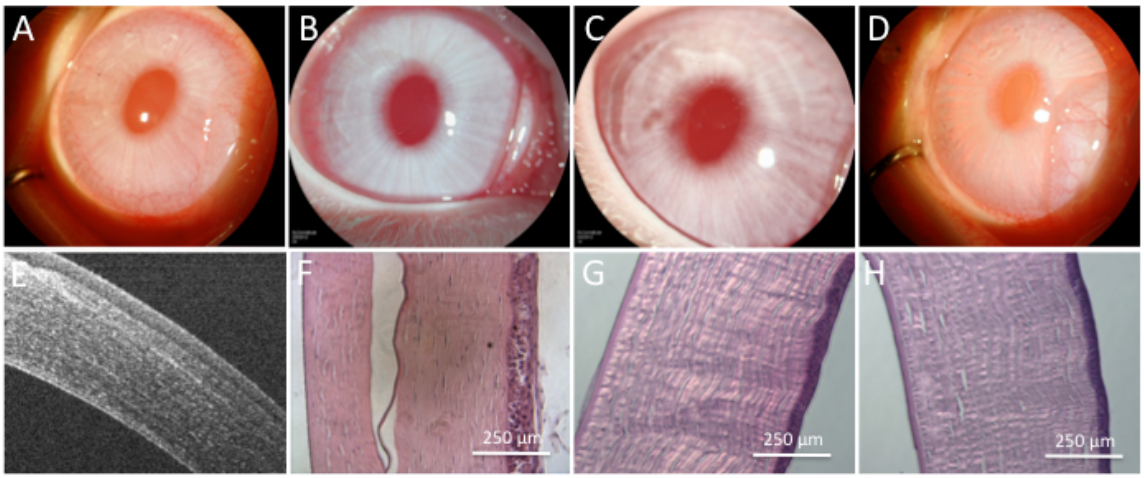

Figure 13. Intrastromal silk film implants in the rabbit cornea. Slit lamp photographs at (A) 1, (B) 6, and (C) 12 weeks post-surgery, and (D) control at 12 weeks. (E) OCT image of cornea at 12 weeks post-op demonstrating absence of inflammatory cells. H&E staining of cornea cross-sections at (F) 6 and (G) 12 weeks post implantation, and (H) control at 12 weeks.

2.4.2: Assessment of silk bandage puncture wound covering capability

In some circumstances after an ocular injury incident a puncture wound that perforates the cornea may occur. In addition, surgical interventions such as cataract surgery or intravitreal injection procedures will puncture the ocular surface. In these circumstances it would be beneficial to cover the wound site to prevent further exposure to injury, while

also ensuring that external pathogens will not enter the intraocular space. The silk bandage's ability to cover a puncture wound site was assessed on an explanted porcine eye model.

Intraocular pressure (IOP) was manually adjusted within the explanted eyes to increase pressure until the leakage occurred at the puncture wound site. Selected eyes were either used as untreated controls or the puncture wound site was covered with a silk bandage. In order to determine if the silk bandage was covering the wound site effectively Indian ink dye was applied over the injury site, and then allowed to incubate upon the eye surface for 1 minute to allow for the potential of ink migration into the wound site. The eyes were then rinsed with saline solution, and the injury sites were explanted for fixation and histological examination.

The explanted tissue was fixed in 4% paraformaldehyde at 4°C for overnight, and then washed three times with saline solution. The tissue was then mounted in paraffin blocks, and then sectioned for Hemotoxylin and eosin (H&E) staining. Sections from both control and silk bandage treated eyes were analyzed using optical microscopy (Figure 14). The puncture wound in both groups appeared as a distinctively disrupted region of the tissue section, and Indian ink showed in black contrast. It was noted that silk bandage treated samples appeared to enhance the entrance of Indian ink into the wound site (Figure 14A) when compared to untreated controls (Figure 14B). This result indicates the silk bandage may increase particle penetration into the wound site as it absorbs the applied Indian ink particles and then dissolves upon the puncture wound. These results may indicate that silk bandage will absorb and then help redeposit molecules upon a wound area. Such properties may be beneficial in regards to enhancing delivery of drugs, such as antibiotics or anesthetics, upon the eye to increase dosing effectiveness and prolonging exposure response. However, the data also indicates the silk bandage does not produce wound-sealing characteristics. As a result of these initial experiments it can be inferred that a significant redesign of the bandage may be required to offer wound-sealing characteristics, however the current design does lend itself as a drug delivery vehicle.

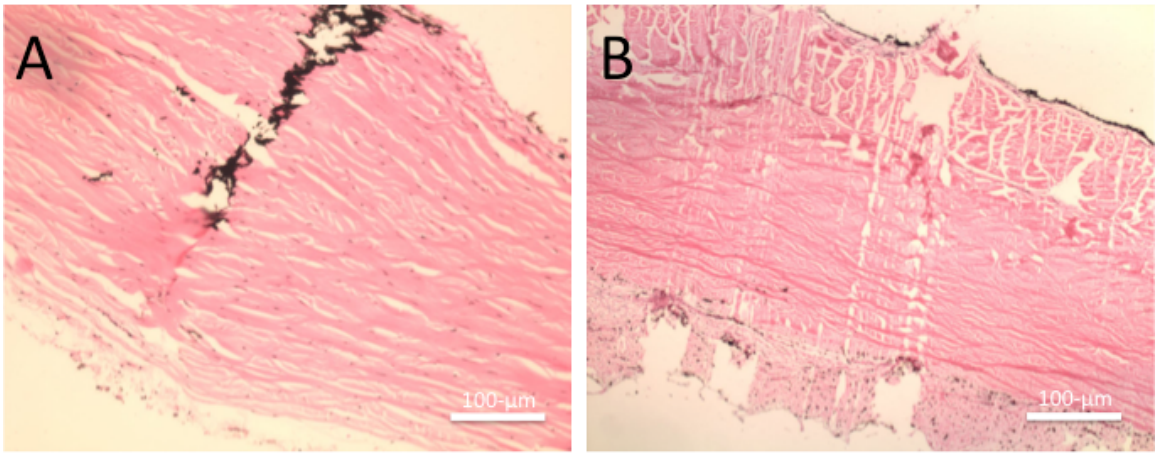

Figure 14. Histological sections of explanted porcine cornea tissue showing the puncture wound injury site for a (A) silk bandage treated, and (B) untreated control. The black coloring represents Indian ink particles, which in the case of the silk bandage covered eye has ingressed into the puncture wound.

2.4.3: *In vivo* trials summary and incorporation of hyaluronic acid (HA)

The above epithelial debridement studies brought to light a number of unanticipated issues regarding the silk bandage design. Firstly, the silk bandage appeared to have a mucoadhesive nature that slowed the blinking response and appeared to be “sticking” to the eyelid after application. In addition, it was noted that bandages that lasted longer than 30 minutes on the corneal surface became insoluble, and could potentially abrade the ocular surface and cause damage. As a result, a redesign of the silk bandage product was considered and implemented in an in vivo rabbit model. Of primary concern was that the silk bandage product has not meeting expected corneal dissolution time and lubricity requirements upon the ocular surface. As a result a silk bandage was formulated that incorporated hyaluronic acid (HA), which is known to be highly miscible with silk fibroin protein and add lubricating properties to the blended material combination (*9*). The silk/HA blending approach was an attempt to both enhance corneal residence time and improve material lubricious properties.

Initial in vitro results suggested that bandage dissolution time was not readily extended with HA incorporation, however the combined materials provided a lubricious surface and produced a more flexible material. As a result *in vivo* rabbit cornea residence time trials were undertaken to assess the response of the corneal surface to the combined material bandage product. Results indicated that the HA appeared to expedite dissolution time upon the corneal surface, where bandages dissolved within 15

minutes after application. Although dissolution time was reduced, it was found that the bandages were easier to apply to the corneal surface due to their enhanced flexibility. In addition, the material wetted more uniformly on the corneal surface when compared to silk alone, and were less “wrinkled” in nature. Finally, it was noted that the eyelid slid more easily across the silk/HA blended bandages due to the materials enhanced lubricity.

Results from this phase of animal trials indicated that silk fibroin could be successfully blended with HA to produce a corneal bandage with enhanced lubricious and mechanical properties. However, an increase in residence time was not achieved. Water-annealing processing was found to impact material solubility significantly, in that such processing produced insoluble blended bandages. However, these initial observations will require more work to determine if such processing can be used to produce a desired dissolution response. From the combination of current and previous data it is unclear if it will be possible to reach the expected corneal residence time of several hours.

2.5: Task 5: GMP-grade production of silk solution

2.5.1. GMP production of silk solution

Silk solution is produced through a series of processing steps, which dissolve silkworm cocoons into an aqueous protein solution (*10*). The variability in producing silk solution has been a significant challenge for translating this biomaterial into product form (*11*). During this award period significant progress was made towards translating silk bandage development from the research laboratory bench to a GMP compliant manufacturing process. Current lab protocols introduce non-satisfactory levels of variability into the silk solution production process. Great effort was undertaken to redesign the silk solution production process to minimize direct user interaction, and produce a more consistent product batch to batch that is also straightforward to validate and reproduce.

In order to accomplish this task two separate systems were designed and implemented within a ISO 6 clean room setting. The first system (Figure 15A) produces extracted silk fibroin fibers from raw silk worm cocoons, and the second system (Figure 15B) allows for automated dialysis to remove the dissolution salts (i.e. lithium bromide). The PLC controllers for both units allow for push button start to finish processing while

supplying a consistent batch-to-batch production with real-time monitoring of the silk production process.

The implementation of both systems has resulted in an order of magnitude increase in silk solution production capability compared to lab-based methods, and has also allowed for greater control over the extraction process through the addition of high precision heating controls and water handling. Previous laboratory setups typically yielded 50 mL of 8% wt./vol. silk solution product over a two-day process. The new system can now produce 700 mL over the same time period, and utilizes similar labor requirements. As a result of this increased manufacturing capacity the company is better positioned to meet potential future demand, while also significantly reducing production costs.

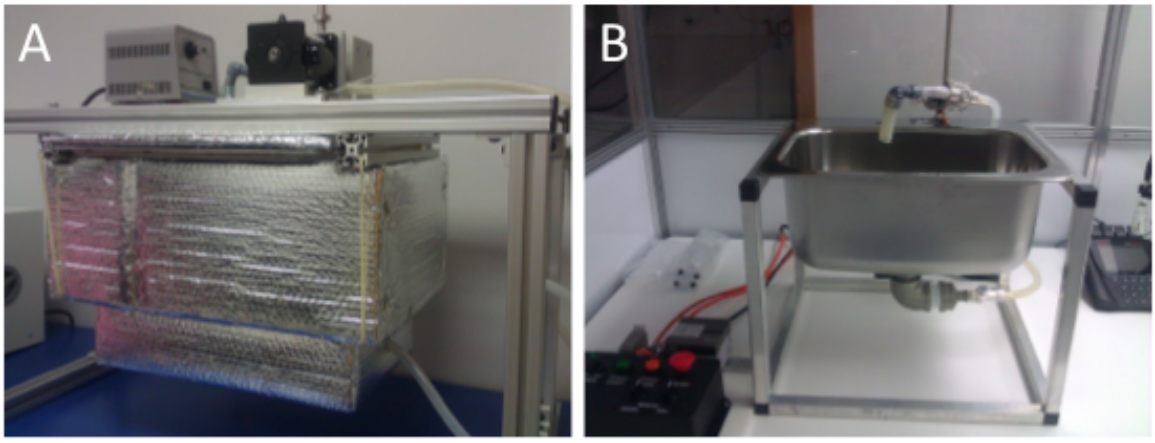

Figure 15. (A) Silk extraction and (B) dialysis systems. Implementation of these fully scalable systems have increased manufacturing capacity by over 10-fold and reduced production costs significantly, while simultaneously allowing for decreased batch-to-batch variability.

Additionally, the system redesign has allowed the implementation of more precise control and monitoring over the batch production process. Specifically, a controlled recirculating heating element has been added to the PLC that allows for greater control over the system's temperature and dwell times during the extraction process. The system has also been insulated that allows for a predictable linear increase in water heating temperature and time, which further adds to batch consistency (Figure 16A). Monitoring elements have been included to allow for real time monitoring of pH (Figure 16B), lithium bromide concentration, temperature, and conductivity during the extraction process to enable quality control logging of batch processing parameters.

The system has also been designed to handle varying batch sizes that range from 5 – 50 grams of silkworm cocoons. Such adaptability enables a significant range of batch size that can be utilized for a specific production need, such as an R&D run or full production, and aids in the elimination of wasted water, energy, chemicals, and operator time. Further work will validate and implement an ISO certified quality system surrounding these systems.

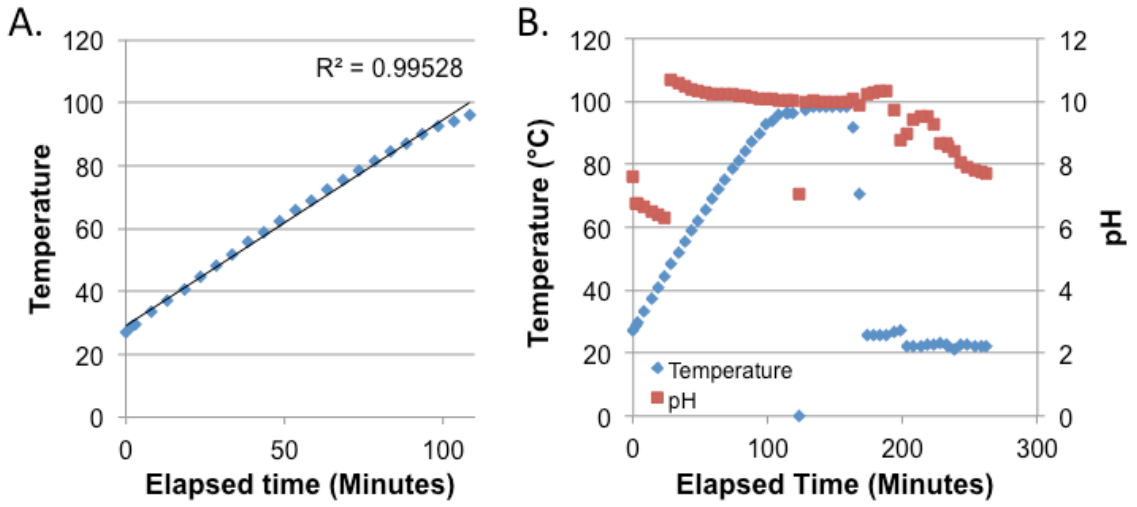

Figure 16. (A) Linear heating of the extraction system water bath is achieved, which allows for enhanced silk processing predictability and reduces batch-to-batch variability. (B) Both pH and temperature are monitored in real-time during each batch run, and the effect of chemical additives on the process can be adjusted as required.

2.5.2: Producing a shaped silk film bandage

A flat silk bandage will not conform to the ocular surface, making it difficult to get the film to readily adhere to the corneal surface uniformly. This could cause potential discomfort to the animal and also affect the outcomes of the study due to non-uniformity in film coverage over the cornea area. As a result a silk bandage with a curve shape was designed and a system was implemented for production. The spin casting process has been used to create standard contact lenses in the past and was a good candidate technique for shaping silk films. A spin casting process was developed within the lab that could consistently produce curved silk bandages (Figure 17). A scalable spin casting system was built in which a curved silicone rubber mold could be mounted onto spindles connected to a variable speed motor through a power transfer belt system. The latest version of the device can produce 20 silk bandages per batch. Briefly, 70 uL of

silk solution is pipetted into the curved silicone rubber molds and then the spun at a fixed rate for a specified period of time until the solution dried. The dried curved film can then be easily removed by bending the silicone rubber mold and air-lifting the curved film from the casting surface. The films that emerge are both curved in shape and are highly transparent. The process was found to be highly reproducible and silk film dimensions were easily controlled by spin cast process parameter optimization (i.e. air flow, RPM, and silk concentration).

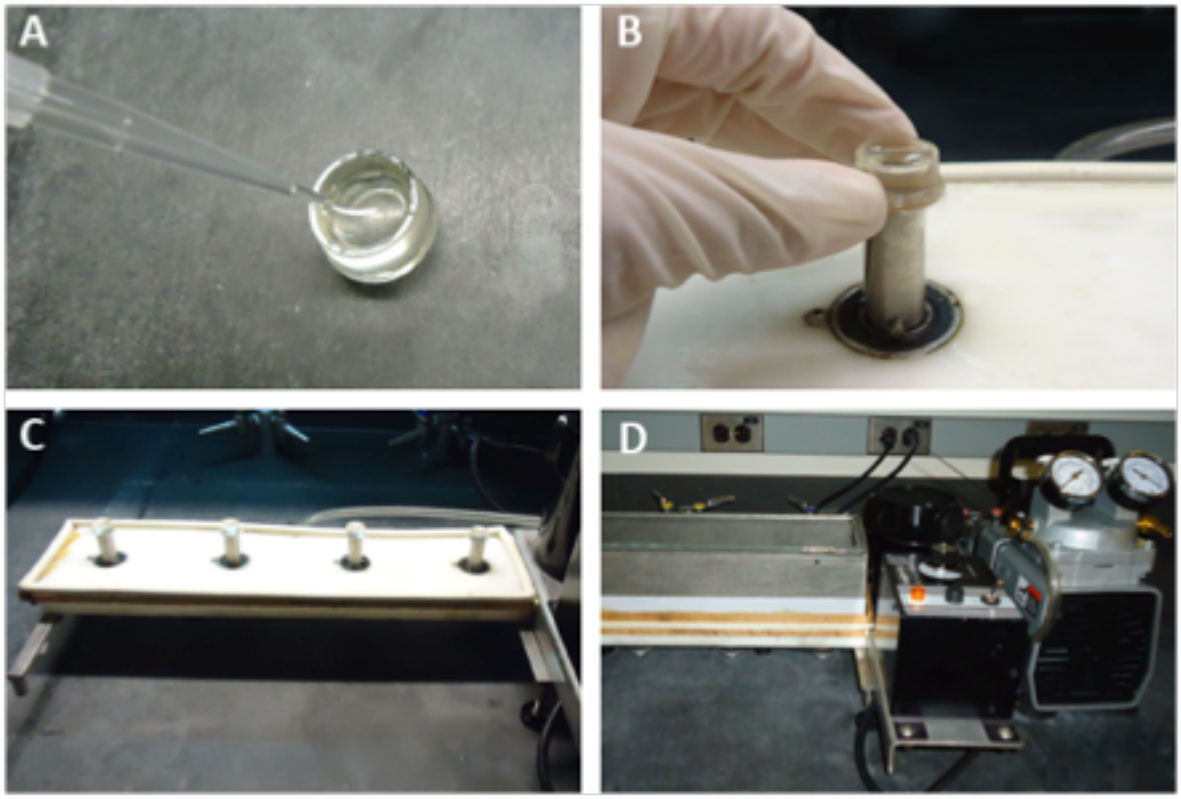

Figure 17. (A) Silk solution is cast into a curved silicone rubber mold and (B) then mounted onto a spindle and rotated at a controlled rate. (C) Lab prototype containing 4 spin casting spindles. (D) The spin casting area was covered, the spindles were attached to a variable voltage motor, and a compressor was used to provide a controlled pressurized source of convective air-flow through the chamber.

Manufacturing parameters were studied to better understand how silk film shape and uniformity may be controlled for a desired material design. The concentration of the silk solution was determined to be an important factor in producing a uniform shaped silk film. It was found that solutions containing to low of silk protein concentration had

significant problems in wetting the silicone rubber surface during the spin cast process when compared to higher concentrated silk solution, which produced a uniform and well shaped curved silk film bandage. The low silk concentration creates irregularly shaped formations in comparison to those made from the higher silk solution concentration (Figure 18).

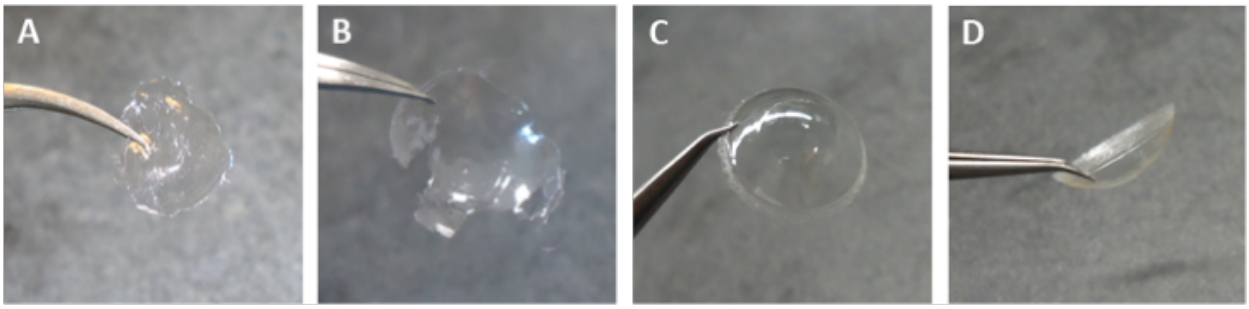

Figure 18. Silk films spin casted using (A)(B) low silk solution concentration and those produced using (C)(D) high silk solution concentration. Silk film bandages produced with high silk solution showed uniform film formation and curvature when compared to the reduced silk concentration, which did not form complete curved body.

The casting chamber was also vented with pressurized air to reduce silk solution drying time. It was shown that the introduction of air-flow reduced drying time in half (Figure 19A). The addition of the pressurized air showed significant effects on silk film bandage thickness uniformity, however the effect on drying rate was negligible in that as long as vented air was flowing through the system drying time was decreased. It was shown that the higher drying rate produced thinner silk film bandage thickness profiles when compared to various other air pressure settings. More profound was the effect of rotations per minute (RPM) settings on silk film thickness uniformity. It was found that RPM could be optimized to form a uniform silk bandage center to periphery thickness when compared to other selected RPM settings (Figure 19B). Reduced RPM settings produced films with a thicker center thickness and a thinning periphery, while films produced at higher RPMs had relatively thick peripheries and extremely thin, or even nonexistent, center thicknesses (Figure 19C-D).

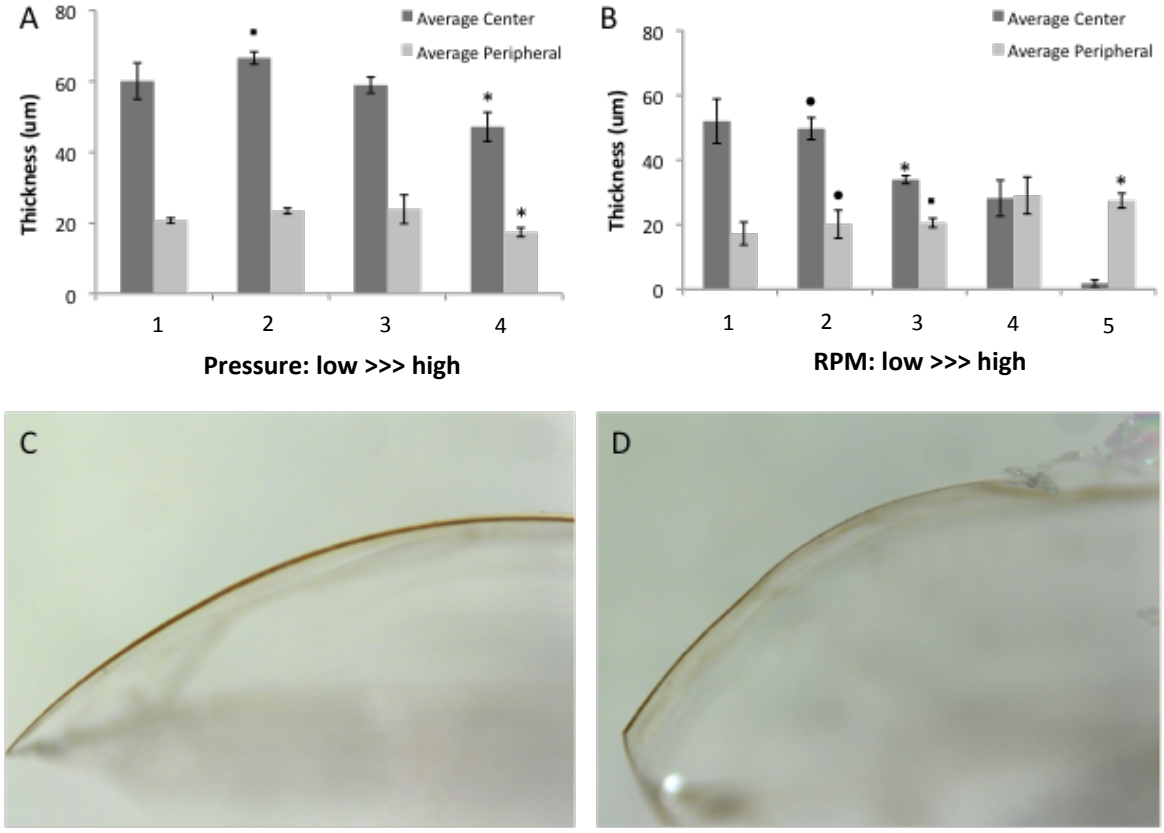

Figure 19. (A) Effects of chamber air pressure on spin casting of shaped silk film thickness for center and periphery areas (n = 4, error bars = standard deviation, * indicates $p < 0.05$ compared to settings 1, 2 & 4 psi. ▪ indicates $p < 0.05$ compared to 1 & 4 settings). (B) Effects of RPM speed of spin casting spindle on silk film bandage thickness for center and periphery areas (n = 4, error bars = standard deviation, * indicates $p < 0.05$ compared to all other speeds except setting 4 in each group. ● indicates $p < 0.05$ when compared to all other speeds except setting 1 in each group. ▪ indicates $p < 0.05$ compared to all 7 other speeds except settings 1 and 2 in each group). Thickness profile images of silk film bandages produced at (C) setting 2 and (D) 5 demonstrating thickness uniformity differences between two spin rates.

2.5.3: E-beam sterilization studies and silk bandage packaging development

Significant advances in product sterilization methodology and packaging were undertaken. Although a number of sterilization procedures have been explored previously (i.e. super-critical CO_2 and dry heat) with some success, these previous methods tended to provide neither inconsistent results or were not standard sterilization methodologies making future validation protocols somewhat difficult to perform from both a technical and financial standpoint. As a result, the highly consistent and validated E-beam sterilization technique was explored. E-beam sterilization utilizes high-energy

electron beams to break the DNA of microorganisms and thus sterilizes the irradiated region. Post-processing analysis of silk samples treated by E-beam with FTIR demonstrated no significant change in protein secondary structure (data not shown), indicating that E-beam does not appear to produce material changes in the silk bandage. Silk dissolution studies in water indicated no significant changes between the E-beam treated and untreated controls (Figure 20A), and illustrates this method offers a potential choice for end-point packaged product sterilization. The packaging design was also completed where the silk bandage product will be placed in a molded plastic base to both assist in handling and protecting the product (Figure 20B). Once the bandage is placed in the plastic molding the combined product and base is placed within a foil pouch, sealed, and sent out for E-beam sterilization.

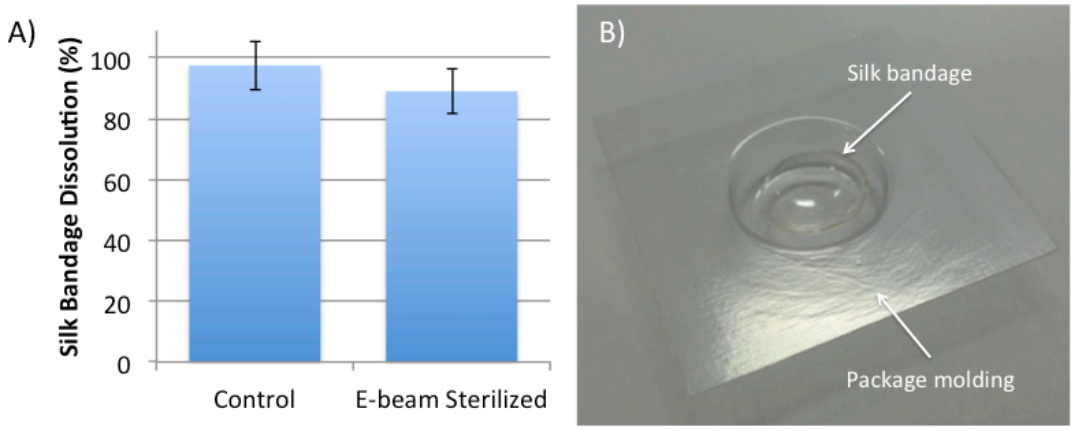

Figure 20. (A) Silk bandage dissolution was verified for samples processed by E-beam sterilization, with no significant differences between processed and unprocessed controls. (B) Formed silk bandage placed within package molding that is then placed in a foil pouch and boxed for E-beam sterilization and shipment.

3.0: Key Research Accomplishments

- Identified silk fibroin protein as non-toxic and non-immunogenic to the ocular surface of rabbits
- Identified silk fibroin protein stimulates wound healing, while simultaneously acting as an anti-inflammatory material
- Identification of novel silk bandage processing techniques to produce a scaffold-like device capable of supporting ocular regeneration after injury.
- Characterized the salient material properties of silk film bandages to promote

corneal repair

- Identified parameters for silk film dissolution, which optimizes corneal healing
- Identified film curvature for proper bandage adherence and designed a novel method to produce curved silk bandage which have better apposition to the corneal surface
- Have begun to create the requisite GMP processes to fabricate films suitable for human use
- Silk material was determined to be non-toxic within the corneal stroma tissue
- Discovered processing controls to modify silk bandage dissolution
- Attained lab and clean room operational space at a GMP facility
- Addition of technical personal to assist in product development
- Designed required systems for controlling the water-annealing process, silk extraction, and silk solution dialysis
- Determined a variety of sterilization modalities for final silk bandage product
- Completed design and implementation of first silk bandage packaging iteration

4.0: Reportable Outcomes

- Peer-reviewed publications in-part supported by award:
  1. Lawrence BD*, Pan Z*, Rosenblatt MI. Silk film topography directs collective epithelial cell migration. PLoS ONE 2012; 7(11): e50190.
  2. Lawrence BD, Pan Z, Liu A, Kaplan DL, Rosenblatt MI. Human corneal limbal epithelial cell response to varying silk film geometric topography in vitro. Acta Biomaterialia 2012; 8: 3732-3743.
  3. Liu J*, Lawrence BD*, Liu A, Schwab IR, Oliveira LA, Rosenblatt MI. Silk fibroin as a biomaterial substrate for corneal epithelial cell sheet generation. IOVS 2012; 53:4130-4138.
  4. Lawrence BD, Pan Z, Weber MD, Kaplan DL, Rosenblatt MI. Silk fibroin film culture system for In Vitro analysis and biomaterial design. J. Vis. Exp. 2012; 62, e3646.
- Conference proceedings supported in-part by award:
  1. Lawrence BD, Pan Z, Rosenblatt MI. Patterned silk films guide collective corneal epithelial cell migration. *BMES* platform session, Atlanta, GA (October 2012).

2. Lawrence BD, Pan Z, Liu A, Rosenblatt MI. Guided vinculin formation using patterned silk film substrates. *ARVO* paper session, Ft. Lauderdale, FL (May 2012).
3. Liu J, Lawrence BD, Liu A, Rosenblatt MI. Silk fibroin as a biomaterial substrate for corneal epithelial cell sheet generation. *ARVO*, Ft. Lauderdale, FL (May 2012).
4. Kang KB, Cole B, Lawrence BD, Liu A, Rosenblatt MI. Morphology and alignment of primary human corneal epithelial cells (HCEC) and a human corneal limbal epithelial (HCLE) cell line on nano- and micropatterned silk films. *ARVO*, Ft. Lauderdale, FL (May 2012).
5. Pan Z, Lawrence BD, Rosenblatt MI. Patterned Silk Films Regulate the Cytoskeletal Dynamics and Gene Expression of Corneal Epithelial Cells. *ARVO*, Ft. Lauderdale, FL (May, 2011).

- PhD attained by Brian Lawrence, now executive and PI at startup company
- Attained license from Tufts University for access to claims regarding the corneal bandage product
- Applied for a license from Cornell University for access to claims regarding the corneal bandage product
- Developed rabbit corneal abrasion, alkali burn, intrastromal implantation, puncture wound, and residence time models for determining the affect of silk materials on and within the ocular surface
- Grant funding in the form of an SBIR phase 2 award was successfully obtained through the NSF in part by the outcomes of this work; a total of $400,000 in private funding was obtained in part by the results of this work through investors
- Funding allowed in-part for the hiring of new CEO for the startup company, 2 full time PhD scientists, 2 engineers, 1 administrative assistant, and 2 interns to date.

5.0: Conclusions

Millions of Americans suffer from painful ocular surface wounds each year (*12*). The most severe wounds can cause loss of eyesight and extreme pain to the suffering patient. Seryx Biomedical's silk bandage has the potential to help heal ocular wounds faster and reduce the risk of vision loss. This regenerative bandage is inexpensive and currently produced for less than a few pennies each. Production is fully scalable to

large quantities and can be easily packaged and distributed in a similar fashion as a contact lens. Furthermore, the biomaterial is novel, patented, and new to the medical device industry. It has the potential to be used in conjunction with a majority of ophthalmic procedures.

Specific to the military, ocular trauma from blast injuries is a common and serious condition resulting in nearly 1/5th of military field evacuations (*13*). There is a critical need to develop materials, which could be used on the battlefield to treat these injuries. Silk-based biomaterials have been identified as a potential candidate biomaterial that can be fabricated to allow for stabilization and healing of these injuries in the acute setting. These materials appear to be quite stable and suitable to use as a field dressing for ocular injuries prior to definitive treatment in a more elaborate ophthalmic care setting. Such treatment may reduce the need for immediate field evacuation, while simultaneously stimulating injury healing and reducing the patient's associated painful symptoms.

Silk biomaterials have been under investigation for their use in the production of medical products for a number of clinical applications (*1*, *14*). In addition, silk materials have recently been identified as an excellent candidate for repairing the corneal surface (*15*, *16*). To produce a more effect silk-based product for treating cornea injuries the work performed in this award identified and implemented critical design parameters, including optimal curvature and dissolution rate, for successful commercial use. These parameters were tested *in vitro* on a human corneal-limbal epithelial cell line (HCLE) and *in vivo* on numerous rabbit animal models. The adoptions of spin-casting techniques were used to fabricate curved silk bandages to create materials with optimized curvature to adhere to the cornea surface. In addition, GMP standards and protocols have been and continue to be put into place to allow for rapid and accurate fabrication of these optimized silk film bandages for use in human clinical trials.

Work over the course of the award period has been pivotal in translating basic laboratory research to a manufactured medical device. The first year of the award offered data demonstrating the proof of concept for the successful design, fabrication, and animal use of the bandage. The second year built off these foundational discoveries to uncover the mechanism of control over the WA process to enabled controlled material residence time on the cornea. More exciting yet has been the transition of technical work from the university environment to a manufacturing facility, which will

enable the production of the bandage for human use over the remainder of the award period. Although, the optimization of the residence time has proven to be difficult and ongoing the discover of the silk protein's stimulatory effects on wound healing and natural ability to act as an anti-inflammatory holds much promise for the biomaterial's use on the ocular surface.

6.0: References

1. G. Altman *et al.*, Silk-based biomaterials, *Biomaterials* **24**, 401–416 (2003).

2. D. W. Kim *et al.*, Enhancement of anti-inflammatory activity of PEP-1-FK506 binding protein by silk fibroin peptide, *J. Microbiol. Biotechnol.* **22**, 494–500 (2012).

3. Q. Garrett *et al.*, Carboxymethyl cellulose stimulates rabbit corneal epithelial wound healing, *Current Eye Research* **33**, 567–573 (2008).

4. W. Lan, A. Petznick, S. Heryati, M. Rifada, L. Tong, Lan: Nuclear Factor-κB: Central Regulator in Ocular Surface Inflammation and Diseases, *The Ocular Surface* **10**, 137–148 (2012).

5. L. Werner, J. Chew, N. Mamalis, Experimental evaluation of ophthalmic devices and solutions using rabbit models, *Veterinary Ophthalmology* **9**, 281–291 (2006).

6. B. Lawrence, M. Cronin-Golomb, I. Georgakoudi, D. Kaplan, F. Omenetto, Bioactive silk protein biomaterial systems for optical devices, *Biomacromolecules* **9**, 1214–1220 (2008).

7. X. Hu *et al.*, Regulation of Silk Material Structure by Temperature-Controlled Water Vapor Annealing, *Biomacromolecules* **12**, 1686–1696 (2011).

8. H. Jin *et al.*, Water‐Stable Silk Films with Reduced β‐Sheet Content, *Advanced Functional Materials* **15**, 1241–1247 (2005).

9. M. Garcia-Fuentes, E. Giger, L. Meinel, H. P. Merkle, The effect of hyaluronic acid on silk fibroin conformation, *Biomaterials* **29**, 633–642 (2008).

10. B. D. Lawrence, Z. Pan, M. D. Weber, D. L. Kaplan, M. I. Rosenblatt, Silk film culture system for in vitro analysis and biomaterial design, *J. Vis. Exp.*, e3646 (2012).

11. L. S. Wray *et al.*, Effect of processing on silk‐based biomaterials: Reproducibility and biocompatibility, *Journal of Biomedical Materials Research Part B: Applied Biomaterials* **99**, 89–101 (2011).

12. J. Whitcher, M. Srinivasan, M. Upadhyay, Corneal blindness: a global perspective, *Bulletin of the World Health Organization* **79**, 214–221 (2001).

13. A. Ari, Eye injuries on the battlefields of Iraq and Afghanistan: public health implications, *Optometry-Journal of the American Optometric …* (2006).

14. C. Vepari, D. Kaplan, Silk as a biomaterial, *Progress in Polymer Science* **32**, 991–1007 (2007).

15. L. J. Bray *et al.*, Human corneal epithelial equivalents constructed on Bombyx mori silk fibroin membranes, *Biomaterials* **32**, 5086–5091 (2011).

16. K. Higa, N. Takeshima, F. Moro, Porous Silk Fibroin Film as a Transparent Carrier for Cultivated Corneal Epithelial Sheets, *Journal of …* (2010).